

UNCLASSIFIED

AD NUMBER: AD0890758

LIMITATION CHANGES

TO:

Approved for public release; distribution is unlimited.

FROM:

Distribution authorized to U.S. Gov't. agencies only; Test and Evaluation; 21 DEC 1971. Other requests shall be referred to Office of Naval Research, Acoustic Program (Code 468), Washington, DC 20360.

AUTHORITY

ONR ltr dtd 29 Aug 1973



SPERRY RAND

INTERIM REPORT

**ANALYSIS OF ACOUSTIC BAFFLES
FOR
UNDERWATER NOISE REDUCTION**

CONTRACT N00014-67-C-0303

Reproduction in whole or in part is permitted for
any purpose of the United States Government.

Prepared for

OFFICE OF NAVAL RESEARCH
DEPARTMENT OF THE NAVY
WASHINGTON, D.C. 20360

SGD-4230-0476
DECEMBER 1971

SPERRY GYROSCOPE DIVISION
GREAT NECK, NEW YORK 11020

FOREWORD

This is an interim report on the study of underwater noise reduction techniques being conducted by the Sperry Division for the Office of Naval Research, Acoustic Programs, under Contract No. N00014-67-C-0303. Included in this report is a description of the work being done on spring-mass type acoustic baffles. Specifically, the effects of rigid and compliant outer plates are analyzed, theoretical results are compared with experimental data, and good agreement is obtained. It is concluded that significant gains can be achieved at the lower frequencies through the use of compliant outer plates in the baffle design.

TABLE OF CONTENTS

<u>Section</u>		<u>Page</u>
1	INTRODUCTION	1-1
2	SPRING-MASS BAFFLES	2-1
	A. Rigid Outer Plates	2-1
	B. Compliant Outer Plates	2-2
3	ANALYSIS OF COMPLIANT SPRING-MASS BAFFLE	3-1
4	RESULTS	4-1
5	REFERENCES	5-1

LIST OF ILLUSTRATIONS

<u>Figure</u>		<u>Page</u>
2-1	Spring-Mass Baffle Configuration Under Hydrostatic Pressure	2-3
2-2	Analytical Model of Spring-Mass Baffle with Rigid Outer Plates	2-4
2-3	Equivalent Circuit of Spring-Mass Baffle with Rigid Outer Plates	2-5
2-4	Analytical Model of Spring-Mass Baffle with Compliant Outer Plates	2-6
3-1	Regions on Surface of Baffle Plate	3-8
3-2	Pattern of A Squares	3-9
3-3	Pattern of C Squares	3-9
3-4	Analytical Model of Baffle Assembly Including Hydrophone Mounting Plate	3-10
4-1	Computed Performance of Spring-Mass Baffle (Rigid Outer Plates)	4-7
4-2	Computed Performance of Spring-Mass Baffle (Compliant Outer Plates) (4 Sheets)	4-8
4-3	Comparison of Computed and Experimental Baffled Hydrophone Response (Depth = 100 Feet)	4-12
4-4	Comparison of Computed and Experimental Baffled Hydrophone Response (Depth = 400 Feet)	4-13
4-5	Comparison of Computed and Experimental Baffled Hydrophone Response (Depth = 700 Feet)	4-14

LIST OF TABLES

<u>Table</u>		<u>Page</u>
3-1	Forms of Z_{mn} and P_{mn} $W_{mn}^2 = k^2 - q^2 (m^2 + n^2)$	3-7
3-2	Basic Equations of Motion	3-7
4-1	Program Listing	4-3

SECTION 1

INTRODUCTION

Baffles are structures that shield acoustic sensors from unwanted noise sources and provide means for modifying the response characteristics of hydrophones. Thus, the acoustic baffle is a primary tool for underwater noise reduction and directivity pattern control in sonar arrays.

The transmission of acoustic energy in water can be impeded by a compliant baffle. To be effective, such a baffle must be sufficiently stiff to withstand hydrostatic pressures, yet it should be dynamically soft to perform as a highly reflective structure. A reflective characteristic is acceptable for the side of the baffle facing the interfering noise source, but the portion facing the hydrophone presents a major design challenge. Unless this side is nonreflective, the interaction between the incident signal and the reflected signal from the baffle can alter the hydrophone array's response, often seriously degrading it.

In previous phases of this program, Sperry has developed a set of analytical models for predicting the reflectivity, transmittivity, and other acoustic parameters of planar multilayered baffle structures. Computer programs based on the analytical models have been utilized for determining baffled hydrophone response. The results of this program have shown high correlation with empirical data (References 1 and 2).

More recent work has been concerned with multilayer cylindrical baffles. Analytical expressions have been developed for the calculation of sound pressure level at any point exterior to the baffle, and a computer program to solve these equations was written. The calculated results show good agreement with experimental data (Reference 3).

Additional analysis has been done on baffle structures consisting of steel plates separated by pins. These structures are non-homogeneous and thus cannot be analyzed by the methods previously used. Lumped-parameter models, designed to simulate the behaviour of spring-mass baffles, have been developed. Performance calculations have been made which give good agreement with measured values (Reference 3).

Spring-mass baffles, by proper choice of spring and plate constants, offer the advantage of operating under higher hydrostatic pressures than other types of acoustic baffles.

SECTION 2

SPRING-MASS BAFFLES

A. RIGID OUTER PLATES

A typical spring-mass baffle configuration consisting of four plates is shown in figure 2-1. The outer plates are of moderate thickness and remain effectively rigid under pressure. These plates transmit the pressure, via pins, to the relatively thin inner plates that deform sufficiently to create the desired baffle compliance. The baffle structure is placed behind a heavy steel plate that supports the hydrophones and provides means for modifying their response characteristics.

The schematic representation shown in figure 2-2 illustrates how the analytical model of the baffle was developed.

The analysis was based on the premise that each of the non-deflecting outer plates is rigidly coupled to half of an inner plate which can deform. This mass is then linked by a spring to the other half of the inner plate; the two inner plate halves are rigidly linked together. Mass M_1 represents the mass of plate No. 1 plus half of plate No. 2. Mass m equals the sum of the halves of plates No. 2 and No. 3, while Mass M_2 represents the remaining half of plate No. 3 plus plate No. 4.

Based on the above model, an equivalent circuit of the spring-mass baffle has been developed and is shown in figure 2-3. L represents the associated viscous resistance of the springs, which is due mainly to the rubber pads associated with the separating pins. The characteristic impedance of the water, Z , is numerically equal to 5.84 in an inch-pound-second system. Because of the symmetrical construction of the baffle, $M_1 = M_2 = M$ and $K_1 = K_2 = K$.

An examination of this circuit shows that at the lower frequencies, the effect of the outer plate mass is not significant because the term $-j\omega M$ is much less than the value of Z . In this frequency region, the insertion loss is dominated by the spring term jK/W and thus rises at 6 dB per octave. As the frequency increases, the dissipative term, L , dominates and the insertion loss flattens. At still higher frequencies, the mass terms become significant and the insertion loss again begins to rise.

B. COMPLIANT OUTER PLATES

The performance of the spring-mass baffle has been extended to lower frequencies. Conceptually, this calls for greater compliance in the interior plate-springs of the baffle, which might be obtained by adding further layers of these plate-springs. However, as was noted previously, additional compliance can be obtained, without increasing the baffle thickness, by making the outer plates thinner and thus less rigid.

An improved model for calculating baffle performance has been developed that realistically allows for the deformation of the outer plates. The model described in Section 2A assumes that the outer plates do not deform. The modified model approximates the deformation of the outer plates by dividing them into three regions and allowing each region to be displaced by a spring-like action from the adjacent region. (See figure 2-4.) One region encompasses the area of the outer plate which is linked by pins to the inner plate deformed in one direction. The second region, of equal area to the first, covers the area linked by pins to the inner plate deformed in the opposite direction. The various regions are linked by springs. Section 3 presents the detailed analysis of the compliant outer plate baffle model.

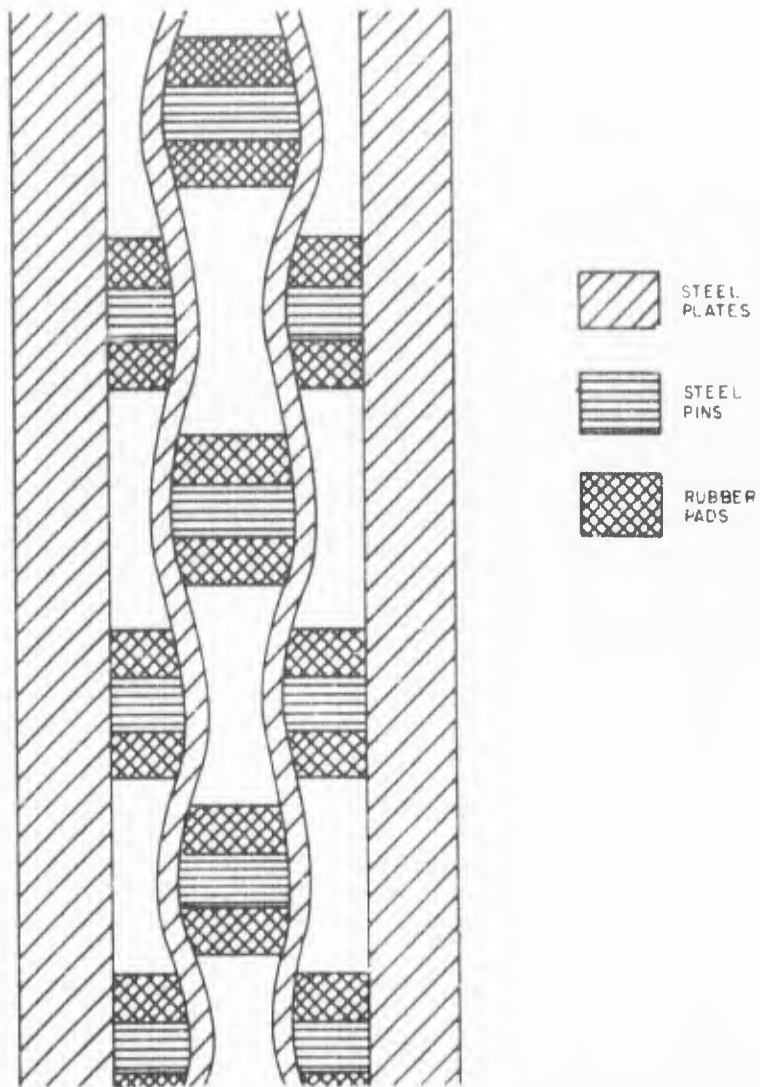


Figure 2-1. Spring-Mass Baffle Configuration Under Hydrostatic Pressure

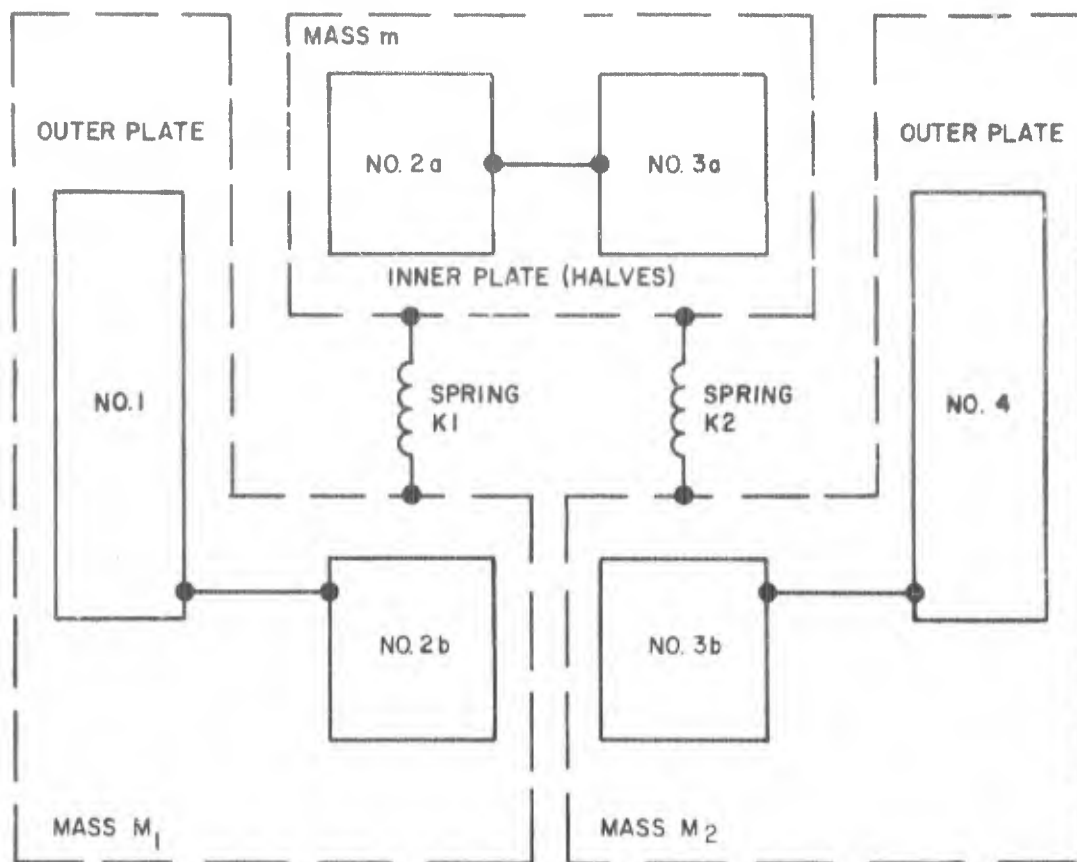


Figure 2-2. Analytical Model of Spring-Mass Baffle with Rigid Outer Plates

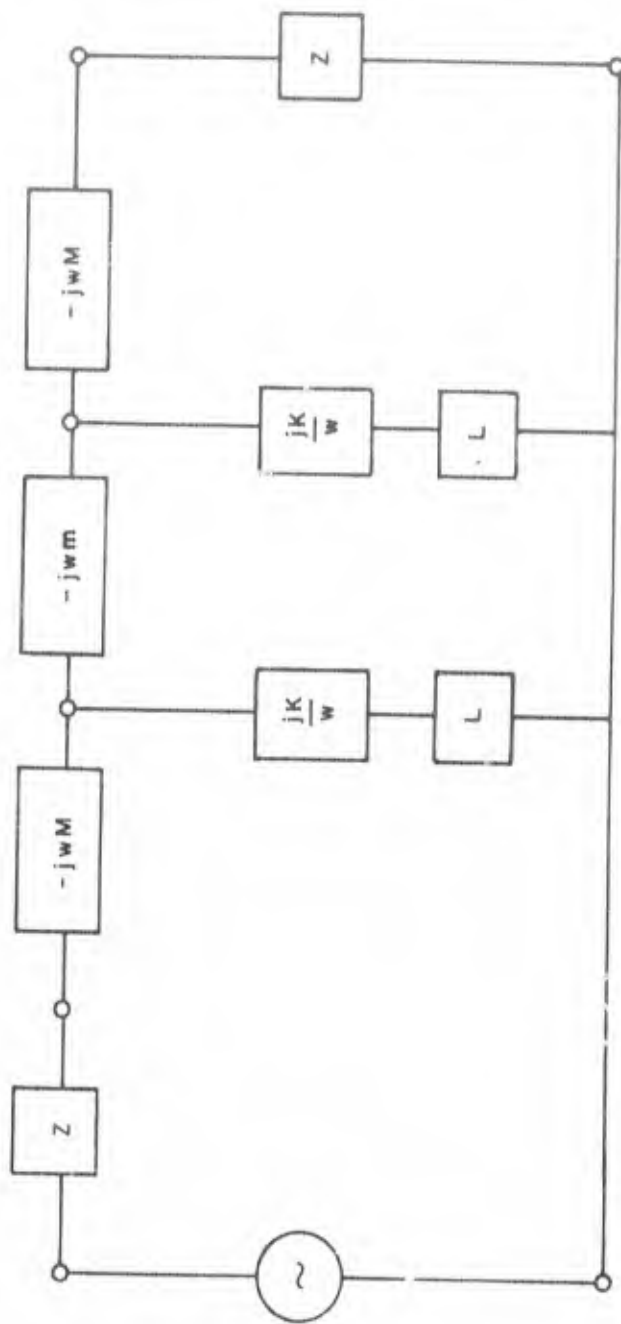


Figure 2-3. Equivalent Circuit of Spring-Mass Baffle with Rigid Outer Plates

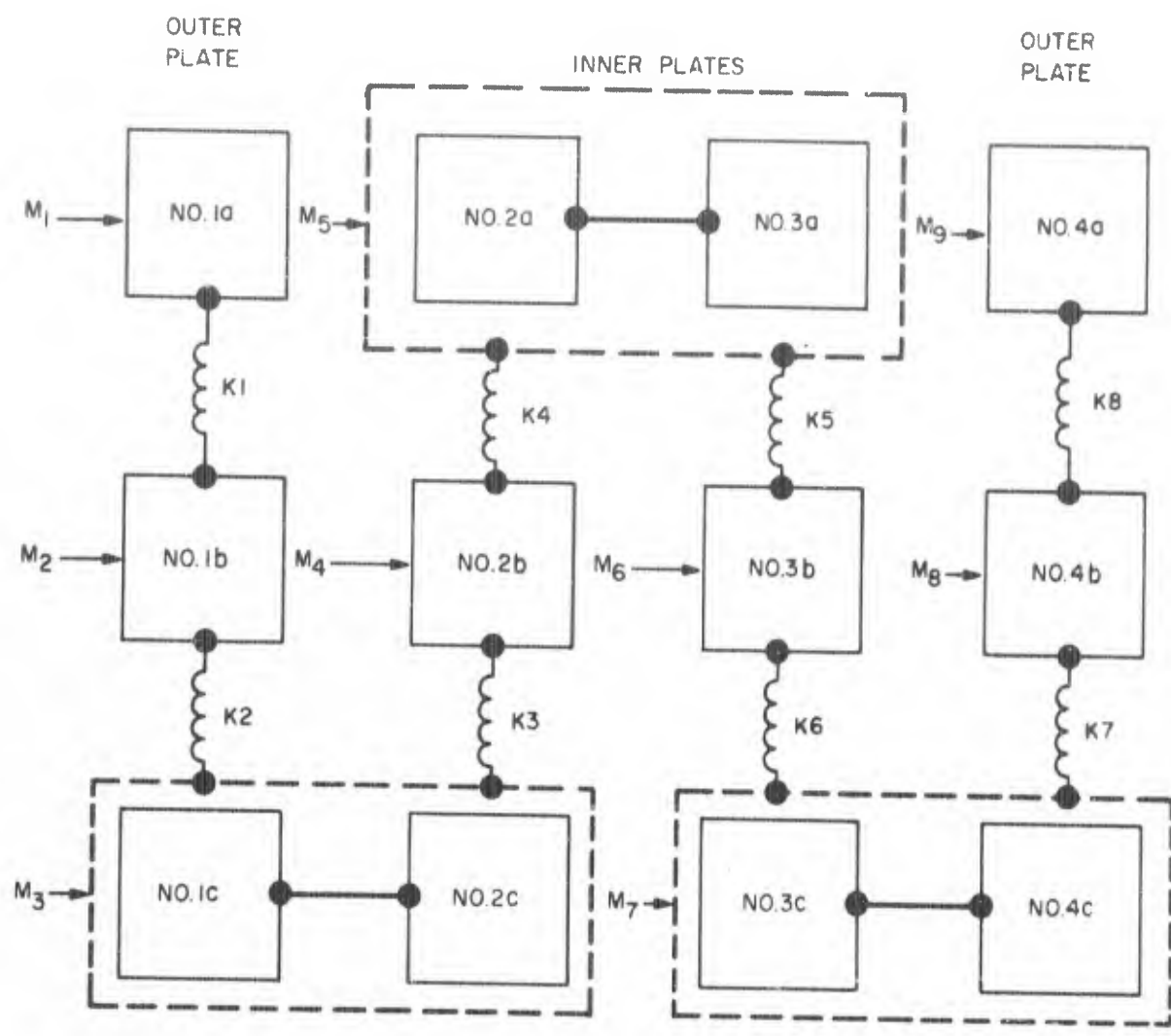


Figure 2-4. Analytical Model of Spring-Mass Baffle with Compliant Outer Plates

SECTION 3

ANALYSIS OF COMPLIANT SPRING-MASS BAFFLE

The area of each baffle plate is divided into three regions as shown in figure 3-1. The interiors of the squares marked A constitute region A, the interiors of the squares marked C constitute region C, and the area exterior to the squares constitutes region B. The centers of the A squares lie over the pins supporting the plate from below; if the plate supports another set of pins, these stand on the C squares. The squares are of such a size that region A and region C each constitute 25 percent of the plate area. Each region has its own amplitude and phase of vibration normal to the plane of the plate. The complex velocities of these vibrations will be denoted by VA, VB, and VC, respectively.

To study the interaction between the vibrating plate and sound waves in the adjacent water, the velocity at the plate surface will be expanded in the form

$$\sum \sum V_{mn} e^{iq (mx + ny)}$$

where $q = \pi/(2^{1/2}d)$ and d is the side of the squares as shown in figure 3-1. The first step is to expand the characteristic functions of regions A and C. (The characteristic function of a region equals 1 inside the region and 0 outside.)

Let the origin be at the center of an A square. A single period of the pattern in figure 3-1, showing only the A squares, has the appearance of figure 3-2. It can be shown that the characteristic function of region A is

$$CFA = (1/4) \sum \sum S_m S_n e^{iq (mx + ny)}$$

where terms having $m + n$ odd are omitted and

$$S_a = \frac{\sin aqd/2}{aqd/2} .$$

When only the C squares are shown, a single period of the pattern in figure 3-1 has the appearance of that shown in figure 3-3. The characteristic function CFC of region C has the same expansion as CFA, except that odd subscript terms are changed in sign.

The velocity at the baffle face may be expressed as

$$V_B + (V_A - V_B) C_{FA} + (V_C - V_B) C_{FC}$$

so that

$$V_{00} = .25 (V_A + 2V_B + V_C),$$

while for even m and n not both zero

$$V_{mn} = .25 (V_A - 2V_B + V_C) S_m S_n$$

and for odd m and n

$$V_{mn} = .25 (V_A - V_C) S_m S_n$$

When $m + n$ is odd, V_{mn} vanishes.

In the water next to the baffle face, the velocity may be expressed as a series

$$V = \sum \sum Z_{mn} e^{iq(mx + ny)}$$

where the coefficients Z_{mn} are functions of z and must satisfy the wave equation

$$Z''/Z = q^2 (m^2 + n^2) - k^2$$

where k is the wave number.

Two kinds of boundary condition will be considered: in the first, the baffle faces a heavy steel plate across a narrow water gap; in the second, the extent of the water is unlimited.

Let the width of the water gap be H and take $z = 0$ at the face of the heavy steel plate, with the positive z -axis pointing toward the baffle. Let Z_{mn} have the form

$$A_{mn} \sin(W_{mn}z) + B_{mn} \cos(W_{mn}z)$$

where $W_{mn}^2 = k^2 - q^2 (m^2 + n^2)$. Both the real and imaginary parts of W_{mn} are assumed non-negative.

Assume that the velocity V_P at the face of the heavy steel plate is independent of x and y . Except for $m = n = 0$, B_{mn} must vanish. Matching velocities at the baffle surface give

$$A_{mn} = V_{mn} \csc(W_{mn}H).$$

The remaining coefficients are given by

$$B_{00} = V_P$$

$$A_{00} = V_{00} \csc(kH) - V_P \cot(kH).$$

For the second kind of boundary condition, let $z = 0$ at the baffle face with the positive z -axis pointing away from the baffle. Express Z_{mn} in the form

$$C_{mn} e^{iW_{mn} z} + D_{mn} e^{-iW_{mn} z}.$$

For positive imaginary W_{mn} , the requirement of boundedness forces D_{mn} to vanish. For positive real W_{mn} , the requirement that any incident wave be planar again forces D_{mn} to vanish unless $m = n = 0$; even then, D_{00} vanishes unless there is an incident wave. Thus D_{mn} vanishes and

$$C_{mn} = V_{mn}$$

except that, if there is an incident wave of (particle) velocity V_I ,

$$D_{00} = V_I$$

$$C_{00} = V_{00} - V_I$$

Table 3-1 summarizes the forms taken by Z_{mn} for various boundary conditions. Also shown are the coefficients in the expansion

$$P = \sum \sum P_{mn} e^{iq (mx + ny)}$$

where P is the pressure in the water. The pressure can be obtained from the velocity using the basic relation

$$\partial P / \partial z = i\omega\rho V$$

The average pressure on an A square can be calculated by integrating P in the x, y , plane. The result is

$$P_A = \sum \sum P_{mn} S_m S_n,$$

with P_{mn} evaluated at the baffle face. The expression for P_C , the average pressure on a C square, is the same except that odd subscript terms are changed in sign. The average pressure P_B on region B is given by the relation

$$P_{00} = .25 (P_A + 2 P_B + P_C).$$

The pressures P_A, P_B, P_C may be expressed in terms of the velocities V_A, V_B, V_C by replacing the coefficients P_{mn} in the pressure expansions by their values taken from table 3-1 and then replacing the V_{mn} by their expressions in terms of the velocities.

The result in the case of the narrow water gap is

$$PA = PH + H2 (VA - 2VB + VC) + H1 (VA - VC)$$

$$PB = PH - H2 (VA - 2VB + VC)$$

$$PC = PH + H2 (VA - 2VB + VC) - H1 (VA - VC)$$

where

$$PH = ic\rho VP \csc (kH) - ic\rho \frac{VA + 2VB + VC}{4} \csc (kH)$$

and H1, H2 are defined as subsums of the series

$$-i\omega\rho .25 \sum \sum (Sm^2 Sn^2 / Wmn) \csc (WmnH).$$

H2 is the sum of all terms having m and n even but not both zero, and H1 is the sum of all terms having m and n odd.

When the water is of unlimited extent, the result is

$$PA = PF + F2 (VA - 2VB + VC) + F1 (VA - VC)$$

$$PB = PF - F2 (VA - 2VB + VC)$$

$$PC = PF + F2 (VA - 2VB + VC) - F1 (VA - VC)$$

where

$$PF = c\rho \frac{VA + 2VB + VC}{4} - 2c\rho VI$$

and F1, F2 are subsums of the series

$$\omega\rho .25 \sum \sum Sm^2 Sn^2 / Wmn.$$

F2 is the sum over terms having m and n even but not both zero, and F1 is the sum over terms having m and n odd.

Equations of Motion

The baffle model to be analyzed is shown in figure 3-4. The mounting plate is optional. Odd-numbered masses represent either single A and C squares of plate or two such squares on adjacent plates, pinned together. Even-numbered masses, except M10, represent plate regions B.

For use in the equations of motion, quantities Mn will represent mass area ratios, the masses all being divided by the area d² of a single A or C square.

The springs shown in figure 3-4 will be characterized by force per volume ratios Kmn equal to the force per unit distance, required to displace mass Mn relative to mass Mn, divided by the area d².

The equations of motion for the 10 masses of figure 3-4 are given in table 3-2. If the mounting plate is not used, the last equation should be omitted. The pressure terms may be eliminated using the pressure/velocity relationships developed above.

At the right end of the assembly, the boundary condition of unlimited water applies so that

$$P_1 = P_F + F_2 (V_1 - 2V_2 + V_3) + F_1 (V_1 - V_3)$$

$$P_2 = P_F - P_2 (V_1 - 2V_2 + V_3)$$

$$P_3 = P_F + F_2 (V_1 - 2V_2 + V_3) - F_1 (V_1 - V_3)$$

where

$$P_F = c\rho \frac{V_1 + 2V_2 + V_3}{4} + 2P_I$$

and $P_I = -c\rho V_I$ is the pressure of the incident wave from the right.

When the mounting plate is not used, the pressures P_7 , P_8 , and P_9 are given by the equations for P_1 , P_2 , and P_3 , respectively, with V_1 , V_2 , and V_3 replaced by $-V_7$, $-V_8$, and $-V_9$, respectively, and P_I replaced by the pressure P_J of the incident wave from the left.

With the mounting plate in place, the boundary condition of the narrow water gap applies at the left end of the assembly, and

$$P_7 = P_H + H_2 (V_7 - 2V_8 + V_9) + H_1 (V_7 - V_9)$$

$$P_8 = P_H - H_2 (V_7 - 2V_8 + V_9)$$

$$P_9 = P_H + H_2 (V_7 - 2V_8 + V_9) - H_1 (V_7 - V_9)$$

where

$$P_H = ic\rho V_{10} \csc(kH) - ic \frac{V_7 + 2V_8 + V_9}{4} \csc(kH).$$

In the last equation of table 3-2, P_{10} is the value of P_{00} at the face of the mounting plate:

$$P_{10} = ic\rho V_{10} \csc(kH) - ic\rho \frac{V_7 + 2V_8 + V_9}{4} \csc(kH).$$

The pressure P_O is related to the incident-wave pressure P_J and the reflected-wave pressure P_R by the equations

$$P_O = P_J + P_R$$

$$c\rho V_{10} = P_J - P_R$$

which show $P_0 = 2P_J - c\rho V_{10}$. This is the quantity to be measured when the mounting plate is in place. With the mounting plate removed, the desired quantity is the value of P_0 at the baffle face. To summarize, the quantities to be measured are:

$$2P_J - c\rho V_{10} \quad (\text{mounted})$$

$$2P_J - c\rho \frac{V_7 + 2V_8 + V_9}{4} \quad (\text{isolated}).$$

TABLE 3-1

FORMS OF Z_{mn} AND P_{mn}
 $W_{mn}^2 = k^2 - q^2 (m^2 + n^2)$

NARROW WATER GAP

$$Z_{mn} = V_{mn} \sin(W_{mn}z) / \sin(W_{mn}H)$$

$$P_{mn} = -i\omega\rho (V_{mn}/W_{mn}) \cos(W_{mn}z) / \sin(W_{mn}H)$$

$$Z_{00} = (V_{00} \csc(kH) - VP \operatorname{ctn}(kH)) \sin(kz) + VP \cos(kz)$$

$$P_{00} = ic\rho VP \sin(kz) - ic\rho (V_{00} \csc(kH) - VP \operatorname{ctn}(kH)) \cos(kz)$$

UNLIMITED WATER

$$Z_{mn} = V_{mn} \exp(iW_{mn}z)$$

$$P_{mn} = \omega\rho (V_{mn}/W_{mn}) \exp(iW_{mn}z)$$

$$Z_{00} = (V_{00} - VI) \exp(ikz) + VI \exp(-ikz)$$

$$P_{00} = c\rho(V_{00} - VI) \exp(ikz) - c\rho VI \exp(-ikz)$$

(if no incident wave, set $VI = 0$)

TABLE 3-2

BASIC EQUATIONS OF MOTION

$$-i\omega M1V1 = iK12/\omega (V2 - V1) - P1$$

$$-i\omega M2V2 = iK23/\omega (V3 - V2) + iK12/\omega (V1 - V2) - 2P2$$

$$-i\omega M3V3 = iK34/\omega (V4 - V3) + iK23/\omega (V2 - V3) - P3$$

$$-i\omega M4V4 = iK45/\omega (V5 - V4) + iK34/\omega (V3 - V4)$$

$$-i\omega M5V5 = iK56/\omega (V6 - V5) + iK45/\omega (V4 - V5)$$

$$-i\omega M6V6 = iK67/\omega (V7 - V6) + iK56/\omega (V5 - V6)$$

$$-i\omega M7V7 = iK78/\omega (V8 - V7) + iK67/\omega (V6 - V7) + P7$$

$$-i\omega M8V8 = iK89/\omega (V9 - V8) + iK78/\omega (V7 - V8) + 2P8$$

$$-i\omega M9V9 = iK89/\omega (V8 - V9) + P9$$

$$-i\omega M10V10 = 4 (P0 - P10)$$

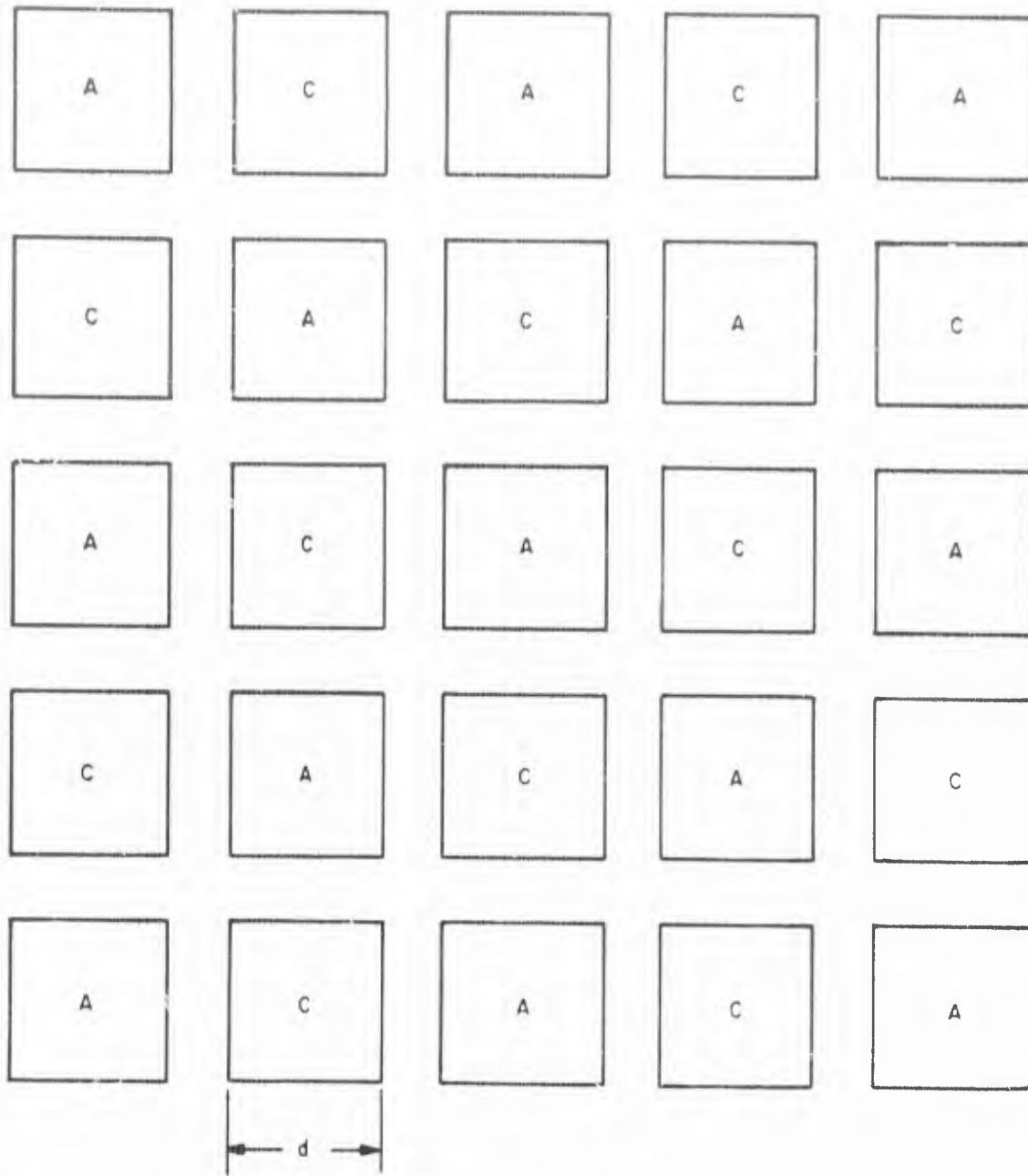


Figure 3-1. Regions on Surface of Baffle Plate

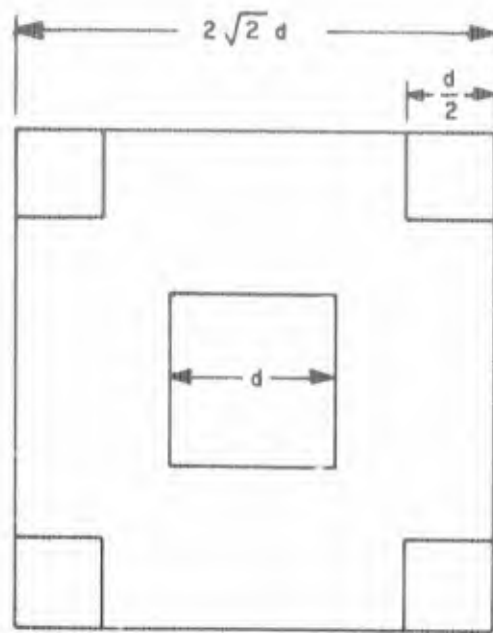


Figure 3-2. Pattern of A Squares

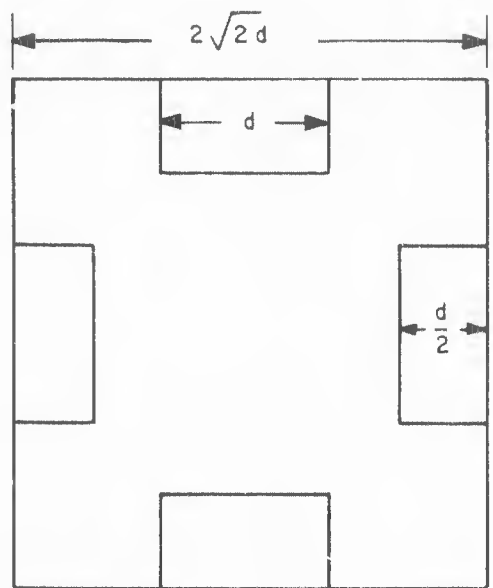


Figure 3-3. Pattern of C Squares

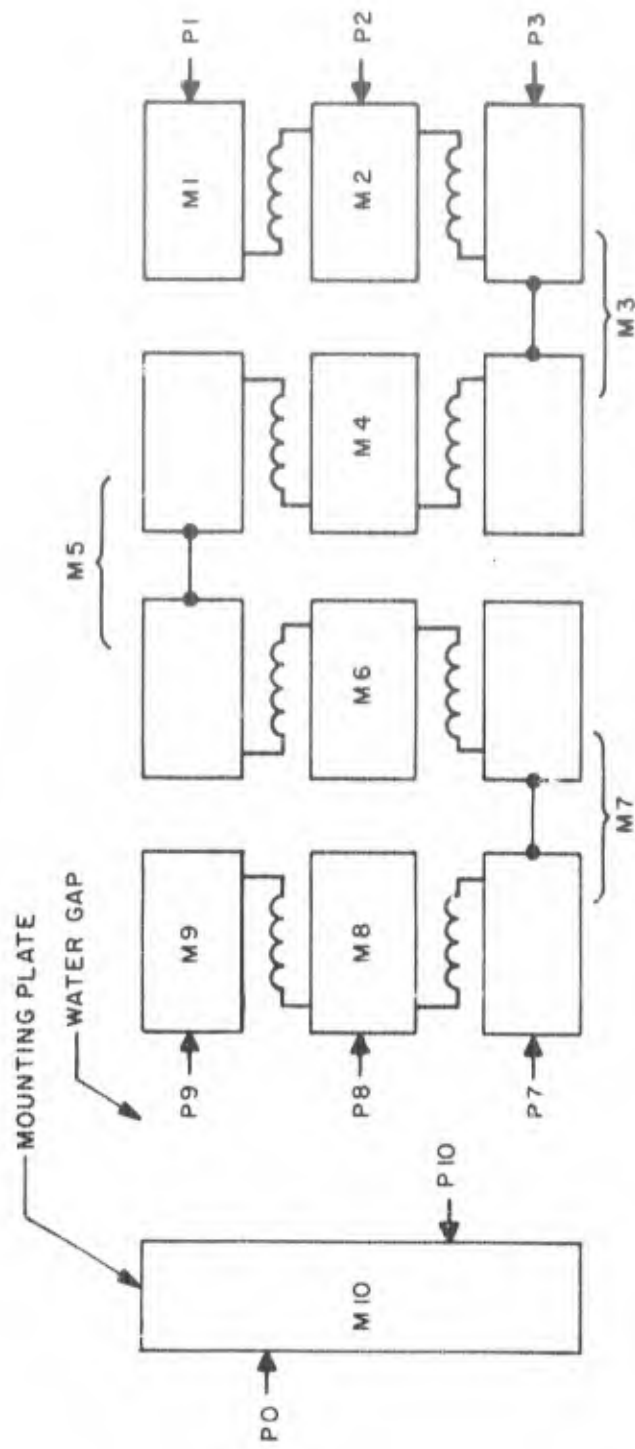


Figure 3-4. Analytical Model of Baffle Assembly Including Hydrophone Mounting Plate

SECTION 4

RESULTS

The equations derived in this report were developed into a computer program and a number of cases were examined. A complete listing of the program is given in table 4-1. The results of the computer runs are illustrated in figures 4-1 and 4-2.

An explanation of the symbols used in the figures is as follows: in all cases the figures pertain to a configuration consisting of a spring-mass baffle mounted a short distance behind a 1-1/2-inch thick steel plate. The plotted points show the pressure at the front of this steel plate as a function of frequency for the two cases of a sound wave incident at the front and the back of the plate-baffle combination. With sound incident from the front, the resulting curve shows the receiving response of a hydrophone mounted on the steel plate. With the sound incident from the back, the resulting curve shows the effectiveness of the baffle in shielding the hydrophone from noise originating behind the baffle. The latter curve is related to insertion loss but is a more practical evaluation of baffle performance since it includes the mounting arrangement for the hydrophone.

In figure 4-1 GAP refers to the distance (in inches) between the steel plate and the baffle. The designations AM, AK and AL pertain to the mass, spring constant and spring damping, respectively, of the masses and springs which comprise the baffle model as shown in figure 2-3. The relatively large mass value (.001104) is that of the 1-1/2-inch steel hydrophone mounting plate. The third spring, whose value is given as 0 in the figures, does not appear in figure 2-3. This spring was placed in the model to account for any compliance between the steel plate and the baffle contributed by the mounting arrangement. It was found in practice, however, that mounting arrangements produce little such compliance. The frequency scale is logarithmic to allow a wide frequency range to be covered on one plot. The reference for 0 dB is the incident sound wave.

In figure 4-2 (4 sheets), the label PIN SPACE refers to the spacing (in inches) between the pins which separate the various plates in the baffle. WATER GAP (in inches) is the distance between the steel plate and the baffle. The MASSES, SPRINGS, and DAMPING are the mechanical parameters of the baffle. The 10 mass values are those for the 10 masses that comprise the baffle model as shown in figure 3-4. Similarly, the eight values for spring constants and damping are for the eight springs in the model. The legend for the plotted points is given at the bottom of the page. Since there are two frequency scales, four curves are needed to display the data. As in the other figures 0 dB is referenced to the level of the incident wave.

Figure 4-1 shows the performance of a baffle in which the outer plates are assumed noncompliant. The mass values correspond to 1/8-inch plastic outer plates and 1/16-inch plastic inner plates. The spring values correspond to operation at low hydrostatic pressures. Note that the crossover point, at which the pressures corresponding to front and back incidence become equal, lies at 45 Hz.

Figure 4-2 (sheet 1 of 4) shows the same configuration, this time analyzed, using the new program written for compliant outer plates, but constrained so as to simulate the original program. Only two of the eight springs are assumed appreciably compliant. As might be expected, the results are effectively the same as in figure 4-1.

Figure 4-2 (sheet 2 of 4) shows the results when two additional springs are allowed to be appreciably compliant, and agrees with figure 4-1. Because of differences in model structure and normalization, the spring and damping parameters are generally eight times as large in the figures generated by the compliant outer plate program than in those generated by the rigid plate program, but the identical physical situation of 1/8-inch plastic outer plates and 1/16-inch inner plates is represented.

Figure 4-2 (sheet 3 of 4) shows the situation when all springs are assumed appreciably compliant. This is the case of compliant outer plates. Since the stiffness varies as the cube of the thickness, the outer plates are eight times as stiff as the inner plates. The insertion loss is improved perhaps by 1 dB at lower frequencies and 4 dB at higher frequencies. Note the dip near 2000 Hz caused by the compliance of the outer plate.

Figure 4-2 (sheet 4 of 4) shows the results for the case where the compliance of the outer plates is increased to match that of the inner plates. Further improvements are evident in the insertion loss, and the dip due to outer-plate compliance has moved down to 700 Hz. From this data it can be concluded that small but definite gains in performance can be made using compliant outer plates in the baffle.

Figures 4-3 through 4-5 compare theoretical data calculated by the compliant outer plate computer program with experimental data obtained from tests of a spring-mass baffle and associated hydrophone array. The array tested consisted of a 6 by 6 foot, 1-1/2-inch thick steel plate in which the hydrophones were mounted; a 1-1/2-inch thick rubber sheet was bonded to the front of the plate, and the spring-mass baffles were placed behind the hydrophone mounting plate.

The figures show the receiving response of the hydrophone mounted in the center of the steel plate at water depths of 100, 400 and 700 feet. The parameters that describe the baffle in the computer program were varied to take into account the effect of depth on the baffle. Agreement at the lower frequencies is very good. At the higher frequencies, the experimental data exhibit ripples which are probably due to the finite size of the array. Especially noteworthy is the correct prediction by the theory of a dip in the response in the vicinity of 4.5 kHz.

TABLE 4-1
PROGRAM LISTING

```

0
01000 PROGRAM BAF111(INPUT,OUTPUT,TAPE1,TAPE6)
01010 DIMENSION DB(64,2,2),DBO(2),FDATA(3,10),FHEAD(7,10)
01020+ ,GLAB(2),IFMT(2),ISCALE(3),ISYM(10),LINE(72),LINREF(72)
01030+ ,LEG(2,2,2),MLAB(2),NF(2),MARK(2,2,2),VAL(10,3),XA(3,3,3)
01040 COMPLEX A(10,12),HF(3,2),Z
01050 COMMON /PARAM/WN,GEOM(2) /SS/SS(50)
01060 DATA PI,CC,RC/3.14159265358979,60630.,5.84/
01070 DATA FDATA/1.84510,.0166667,2.84510, 2.84510,.0166667,3.84510,
01080+ 24*0./
01090 DATA ISCALE/3,0,0/
01100 DATA ISYM/8H11335577,9*0/
01110 DATA XA/1.,0.,-1., 0.,0.,0., -1.,0.,1., 1.,-2.,1., -2.,4.,-2.,
01120+ 1.,-2.,1., 1.,2.,1., 2.,4.,2., 1.,2.,1./
01130 T1 = .5*PI*SQRT(.5) $ SS(1) = 1.
01140 DO 90 N=1,49
01150 90SS(N+1) = (SIN(N*T1)/(N*T1))*2
01160 REWIND 1 $ REWIND 6 $ NPL0T = 0
01170 100READ(1,500) (LINE(L),L=1,8) $ IF(E0F,1) 260,110
01180 500FORMAT(8A10)
01190 110DEC0DE(10,510,LINE) I,J $ IF(I.EQ.1H*) G0T0 100
01200 510FORMAT(3XA1,I1)
01210 G0T0(120,120,120,14),150,260) J
01220* READ MASSES, SPRINGS, DAMPING
01230 120ENC0DE(20,520,IFMT) ISCALE(J)
01240 520FORMAT(1H(,12,17HP,5X311,8(12,F6)))
01250 DEC0DE(80,IFMT,LINE) K,L,M,(N,VAL(N,J),NN=1,K)
01260 IF(L.EQ.0) G0T0 160
01270* SYMMETRY FEATURE IS 0PTIONAL
01280 ENC0DE(10,530,IFMT) ISYM(L)
01290 530FORMAT(A10)
01300 DEC0DE(10,540,IFMT) (LINE(N),N=1,10)
01310 540FORMAT(10I1)
01320 KK = 9-J/2
01330 DO 130 N=1,KK $ NN = LINE(N)
01340 130VAL(N,J) = VAL(NN,J) $ G0T0 160
01350* READ GEOMETRIC DATA
01360 140DEC0DE(80,550,LINE) K,L,M,(N,GEOM(N),NN=1,K) $ G0T0 160
01370 550FORMAT(5X311,2(12,F6))
01380* READ M0DE/PL0T DATA
01390 150DEC0DE(80,560,LINE) NUMF,M0DE,L0GLIN,(NF(N),DRO(N),N=1,NUMF)
01400 560FORMAT(5X311,2(12,F6))
01410 160IF(I.NE.1HE) G0T0 100
01420 NPL0T = NPL0T+1
01430* FREQUENCY L00P
01440 DO 200 NN=1,NUMF $ K = NF(NN)
01450 F1 = FDATA(1,K) $ F2 = FDATA(2,K)
01460 NUMI = 1.5+(FDATA(3,K)-F1)/F2
01470 DO 200 I=1,NUMI
01480 T1 = F1+(I-1)*F2
01490 W = 2.*PI*10.**T1*(2-L0GLIN)+2000.*PI*T1*(L0GLIN-1)
01500 WN = W/CC $ WR = WN*RC
01510 CALL KWIK0(HF)
01520 HF(1,1) = HF(1,1)*CMPLX(0.,WR)
01530 HF(2,1) = HF(2,1)*CMPLX(0.,WR)
01540 HF(3,1) = CMPLX(0.,.25*RC/TAN(WN*GEOM(2)))

```

TABLE 4-1 (Cont'd)
PROGRAM LISTING

```

0
01550 HF(1,2)= HF(1,2)*CMPLX(WR,0.)
01560 HF(2,2)= HF(2,2)*CMPLX(WR,0.)
01570 HF(3,2)= CMPLX(.25*RC,0.)
01580* ENTER MATRIX VALUES
01590 D0 170 J=1,10 $ D0 170 K=1,12
01600 170A(J,K)= (0.,0.)
01610 D0 180 J=1,10 $ IF(J.GT.8) G0T0 180
01620 Z= CMPLX(VAL(J,3),VAL(J,2)/W)
01630 A(J,J)= A(J,J)+Z $ A(J,J+1)= -Z
01640 A(J+1,J+1)= A(J+1,J+1)+Z $ A(J+1,J)= -Z
01650 180A(J,J)= A(J,J)+CMPLX(0.,-W*VAL(J,1))
01660 Z= CMPLX(0.,-RC/SIN(WN*GEOM(2)))
01670 D0 190 J=1,3
01680 A(J,12)= -XA(J,2,3) $ A(J+6,11)= (M0DE-1)*XA(J,2,3)
01690 A(J+6,10)= Z*XA(J,1,3) $ A(10,J+6)= Z*XA(J,1,3)
01700 D0 190 K=1,3 $ D0 190 L=1,3
01710 A(J,K)= A(J,K)+XA(J,K,L)*HF(L,2)
01720 190A(J+6,K+6)= A(J+6,K+6)+XA(J,K,L)*HF(L,M0DE)
01730 A(10,11)= 8. $ A(10,10)= A(10,10)+16.*HF(3,1)+16.*HF(3,2)
01740* FIND PRESSURES
01750 CALL S0LV(A,11-M0DE)
01760 D0 200 J=1,2 $ T1= 4-2*J
01770 Z= T1-RC*((2-M0DE)*A(10,J+10)+(M0DE-1)*.25*(A(7,J+10)
01780+ +2.*A(8,J+10)+A(9,J+10)))
01790 200DB(I,J,NN)= -2000.+2.*AINT(1000.5+10.*AL0G10(CABS(Z)))
01800* PL0T
01810 DATA FHEAD/40H .07 .10 .15 .20 ..
01820+ 24H30 .50 .70,
01830+ 40H .70 1.00 1.50 2.00 3.,
01840+ 24H00 5.00 7.00,56*0./
01850 DATA GLAB/10H PIN SPACE,10H WATER GAP/
01860 DATA (LEG= 10HFR0M FR0NT,10HFR0M BACK,0,0,
01870+ 2(10HFR0M FR0NT,10HFR0M BACK))
01880 DATA MLAB/7HM0UNTED,8HIS0LATED/
01890 DATA MARK/1H+,1H*,0.,),1HX,1H#,1H+,1H*/
01900* WRITE HEADING
01910 I1= 4+NUMF-M0DE $ JJ= 6+M0DE
01920 ENCODE(110,600,LINE) I1,JJ
01930 600F0RMA(10H(4H----12,I1,29)H(/)25X20HPRESSURE AT FR0NT 0F
01940+ 5H/21XA11,25H,21H BAFFLE C0NFIGURATI0N
01950+ 27H/25X19H(DB//INCIDENT WAVE)))
01960 WRITE(6,LINE) NPL0T,MLAB(M0DE)
01970 I1= 3-M0DE $ JJ= 11-M0DE
01980 ENCODE(100,610,LINE) I1,JJ
01990 610F0RMA(1H(11,24H(/26XA10,F6.2)/6HMASSES/12,12H(3PF7.4)/7HS
02000+60HPRINGS/8(OPF7.0)/7HDAMPING/8(OPF7.2)//23X15HFREQUENCY (KHZ)))
02010 WRITE(6,LINE) (GLAB(I),GEOM(I),I=1,I1),(VAL(J,1),J=1,JJ)
02020+ ,(VAL(J,L),J=1,8),L=2,3)
02030 D0 210 I=1,NUMF $ J=NF(I)
02040 ENCODE(70,620,LINE) (FHEAD(K,J),K=1,7)
02050 620F0RMA(7A10)
02060 WRITE(6,630) (LINE(K),K=1,7)
02070 630F0RMA(4X7A10)
02080 DECODE(70,640,LINE) LINE
02090 640F0RMA(70A1)

```

TABLE 4-1 (Cont'd)
PROGRAM LISTING

```

0
02100      D0 210 L=2,70
02110 210 LINREF(L)= LINE(L).AND.(LINE(L).EQ.1H.)
02120      NN= 0 $ KK= NUMF+NUMI $ LL= 2+NUMI
02130      LINE(1)= 4H(DB) $ LINE(LL)= 5H (DB)
02140      T1= DB0(1) $ T2= DB0(2)
02150      ENCODE(20,650,IFMT) NUMI $ GOT0 230
02160      650FORMAT(4H(A5,12,6HA1,A5))
02170*     WRITE ONE LINE (L00P)
02180 220 IF(AMOD(DB0(1),10.).NE.0.) GOT0 230
02190      ENCODE(4,660,LINE) DB0(2) $ LINE(LL)= LINE(1)
02200      660FORMAT(F4.0)
02210      ENCODE(4,660,LINE) DB0(1)
02220 230 D0 240 I=1,NUMI
02230      LINE(I+1)= LINREF(I+1)
02240      IF(LINE(1).NE.0) LINE(I+1)= 1H.
02250      D0 240 J=1,2 $ D0 240 N=1,NUMF
02260      IF(DB(1,J,N).EQ.DB0(N)) LINE(I+1)= MARK(J,N,NUMF)
02270 240 CONTINUE
02280      WRITE(6,IFMT) (LINE(K),K=1,KK)
02290      LINE(1)= ) $ LINE(LL)= 0
02300      DB0(1)= DB0(1)-1. $ DB0(2)= DB0(2)-1.
02310      NN= NN+1 $ IF(NN.LT.36) GOT0 220
02320*     WRITE TAIL
02330      WRITE(6,670)
02340      670FORMAT(
02350      IF(NUMF.EQ.2) WRITE(6,680)
02360      680FORMAT(5X17HUPPER/LEFT SCALE,10X17HLOWER/RIGHT SCALE)
02370      JJ= 5-NUMF $ ENCODE(20,690,LINE) JJ
02380      690FORMAT(28H2(8XA10,1XA1,31XA10,1XA1,7),11,4H(/))
02390+     11,31H(19H INBOARD INCIDENCE A1,16X),11,4H(/))
02400      WRITE(6,LINE) ((LEG(I,J,NUMF),MARK(I,J,NUMF),J=1,2),I=1,2)
02410      DB0(1)= T1 $ DB0(2)= T2 $ GOT0 100
02420*     EXIT
02430 260 WRITE(6,700)
02440      700FORMAT(4H----)
02450      ENDFILE 6 $ REWIND 6
02460      END
08000      SUBROUTINE KWIK0(HF)
08010      COMPLEX HF(3,2)
08020      DIMENSION R(2)
08030      COMMON /PARAM/WN,S,H /SS/SS(50)
08040      DATA ACC,PI/.0001,3.14159265358979/
08050      DATA R/.309325,.088187/
08060      Q= (PI/S)*SQRT(2.) $ QI= 2.*Q**2
08070      HF(1,1)= CMLPX(-R(1)/Q,0.) $ HF(2,1)= CMLPX(-R(2)/Q,0.)
08080      HF(1,2)= CMLPX(0.,-R(1)/Q) $ HF(2,2)= CMLPX(0.,-R(2)/Q)
08090      K= 0 $ IZ= 0 $ E= .75 $ WW= WN*1.E-6
08100 100 K= K+1 $ N= 2
08110      D0 130 II=IZ,K
08120      I= K-II
08130      T1= (2-I/K-(K-I)/K)*SS(K-I+1)*SS(K+1+1)
08140      T3= )*(K**2+I**2)
08150      T2= WN**2-T3 $ T2= SQRT(T2)
08160      IF(T2.LT.0.) GOT0 110
08170      T2= SQRT(T2) $ IF(T2.LT.WW) T2= WW

```

TABLE 4-1 (Cont'd)
PROGRAM LISTING

```

0
08180 HF(N,2)= CMPLX(T1/T2,T1/T3)+HF(N,2)
08190 HF(N,1)= CMPLX(T1/T3+T1/T2/TANH(H*T2),0.)+HF(N,1)
08200 GOT0 120
08210 110T2= SORT(-T2) IF(T2.LT.WN) T2= WN
08220 HF(N,2)= CMPLX(0.,T1/T3-T1/T2)+HF(N,2)
08230 HF(N,1)= CMPLX(T1/T3-T1/T2/TANH(H*T2),0.)+HF(N,1)
08240 120E= E-T1
08250 130N= 3-N
08260 IF(T2.LE.WN) GOT0 100
08270 IF(ABS(E/T3-E/T2/TANH(H*T2))
08280+.GT.ACC*CABS(HF(1,1)+HF(2,1))) GOT0 100
08290 IF(ABS(E/T3-E/T2).GT.ACC*CABS(HF(1,2)+HF(2,2))) GOT0 100
08300 RETURN
08310 END
09000 SUBROUTINE SOLV(A,M)
09010 COMPLEX A(10,12),SUM,T0T
09020 DIMENSION KR(10,2)
09030 DATA KR/1,1,1,3,4,5,6,7,7,7, 3,3,4,5,6,7,10,10,10,10/
09040 D0 150 N=1,M
09050 SUM= (0.,0.)
09060 J1= KR(N,1) $ J2= N-1
09070 IF(J1.GT.J2) GOT0 110
09080 D0 100 J=J1,J2
09090 100SUM= SUM+A(N,J)*A(J,N)
09100 110A(N,N)= 1./CSQRT(A(N,N)-SUM)
09110 K1= N+1 $ K2= MINO(M,KR(N,2))
09120 IF(K1.GT.K2) GOT0 150
09130 D0 140 K=K1,K2
09140 SUM= (0.,0.) $ T0T= (0.,0.)
09150 J1= KR(K,1) $ J2= N-1
09160 IF(J1.GT.J2) GOT0 130
09170 D0 120 J=J1,J2
09180 SUM= SUM+A(K,J)*A(J,N)
09190 120T0T= T0T+A(N,J)*A(J,K)
09200 130A(K,N)= (A(K,N)-SUM)*A(N,N)
09210 140A(N,K)= (A(N,K)-T0T)*A(N,N)
09220 150CONTINUE
09230 D0 170 I=1,12
09240 D0 170 L=1,2
09250 D0 170 K=1,M
09260 SUM= (0.,0.)
09270 N= (2-L)*K +(L-1)*(M+1-K)
09280 J1= (2-L)*KR(N,1)+(L-1)*(N+1)
09290 J2= (2-L)*(N-1) +(L-1)*MINO(M,KR(N,2))
09300 IF(J1.GT.J2) GOT0 170
09310 D0 160 J=J1,J2
09320 160SUM= SUM+A(N,J)*A(J,I)
09330 170A(N,I)= (A(N,I)-SUM)*A(N,N)
09340 RETURN
09350 END

```

LENGTH = 215 LINES

PRESSURE AT FRONT OF
MOUNTED BAFFLE CONFIGURATION
(GAP 2.00)

DB//INCIDENT WAVE
FROM FRONT +
FROM BACK *

AM = .000033 .000016 .000033 .001104
AK = 100 100 0
AL = .300 .300 0.

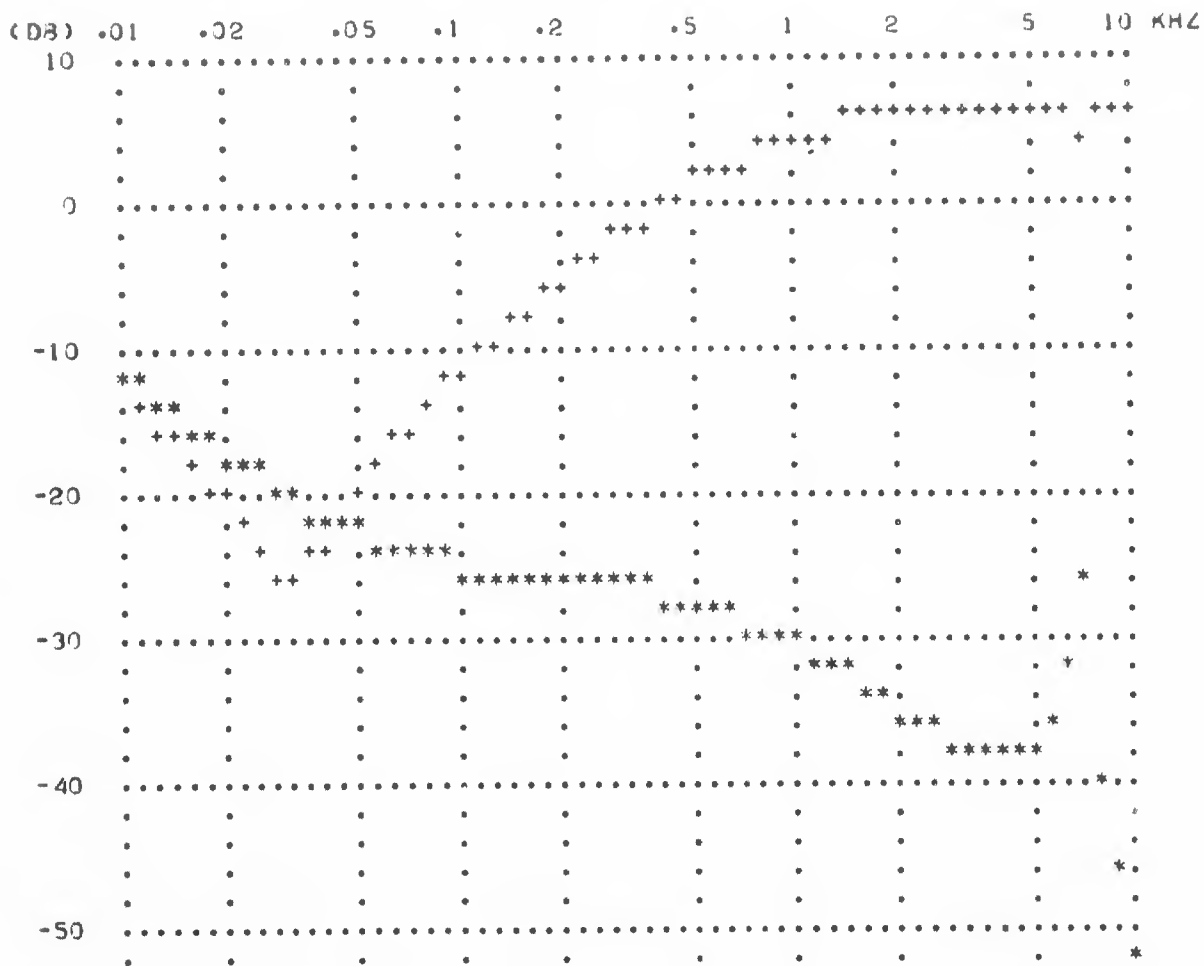
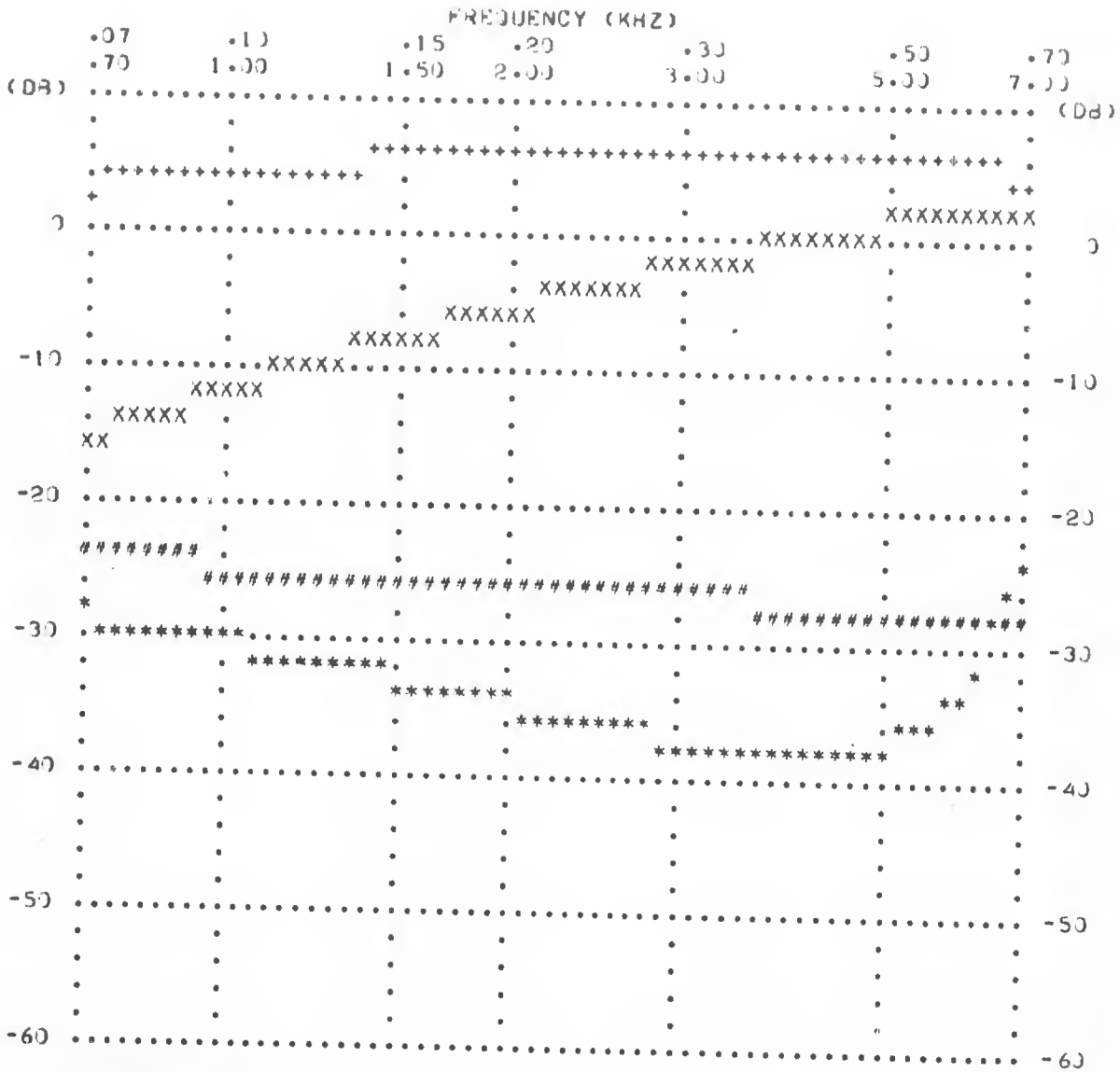


Figure 4-1. Computed Performance of Spring-Mass
Baffle (Rigid Outer Plates)

PRESSURE AT FRONT OF
MOUNTED BAFFLE CONFIGURATION
(DB//INCIDENT WAVE)

PIN SPACE 3.00
WATER GAP 2.00

MASSES	.0233	.0466	.0512	.0233	.0395	.0233	.0512	.0466	.0233	4.4145
SPRINGS	640000	640000	800	800	800	800	640000	640000		
DAMPING	.05	2.40	2.40	2.40	2.40	2.40	2.40	2.40	.05	



UPPER/LEFT SCALES
FROM FRONT X
FROM BACK #

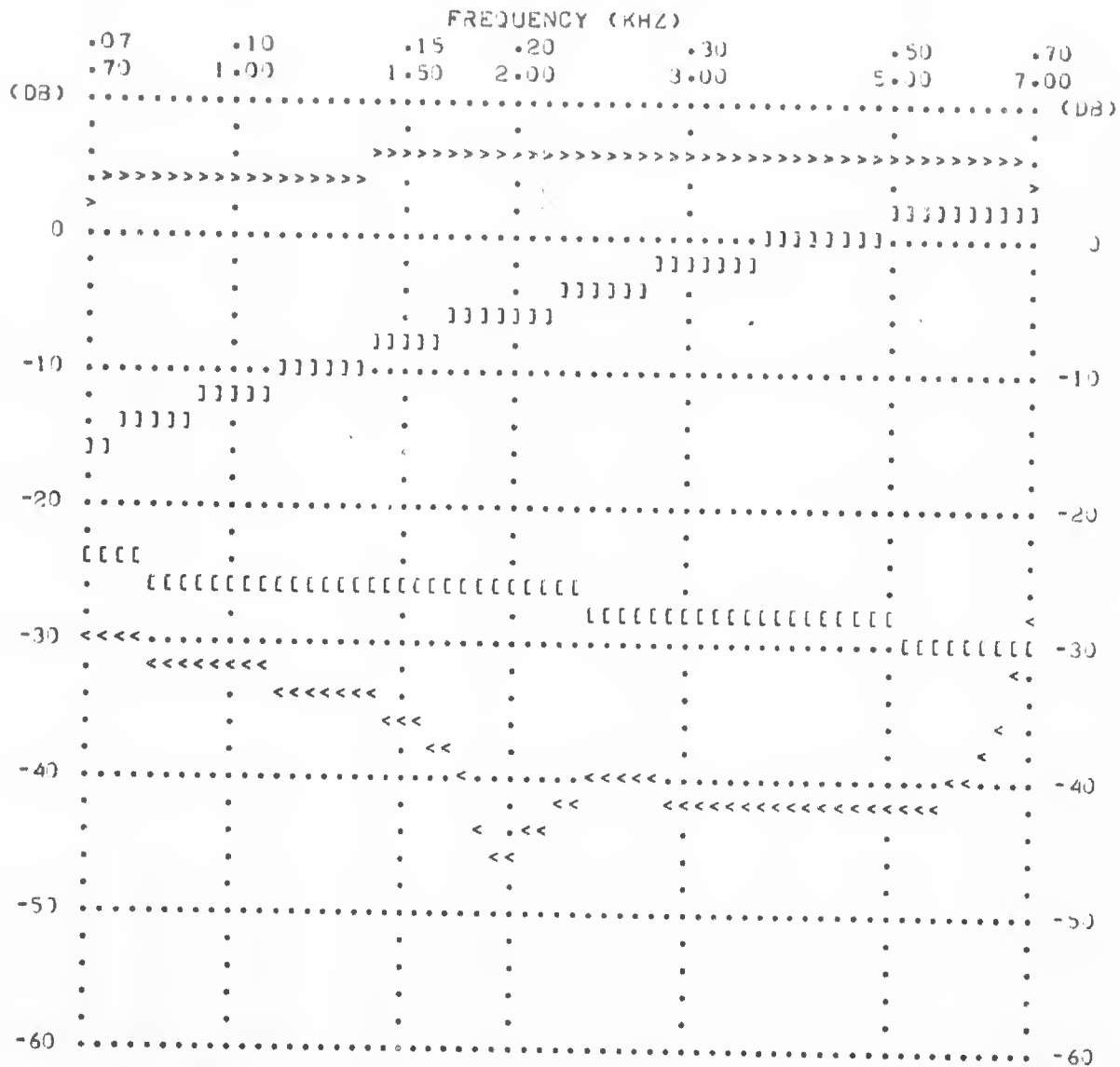
LOWER/RIGHT SCALES
FROM FRONT +
FROM BACK *

Figure 4-2. Computer Performance of Spring-Mass
Baffle (Compliant Outer Plates) (Sheet 2 of 4)

PRESSURE AT FRONT OF
MOUNTED BAFFLE CONFIGURATION
(DB//INCIDENT WAVE)

PIN SPACE 3.00
WATER GAP 2.00

MASSES	.0233	.0466	.0512	.0233	.0395	.0233	.0512	.0466	.0233	4.4145
SPRINGS	6400	6400	800	800	800	800	6400	6400		
DAMPING	.050	2.400	2.400	2.400	2.400	2.400	2.400	.050		



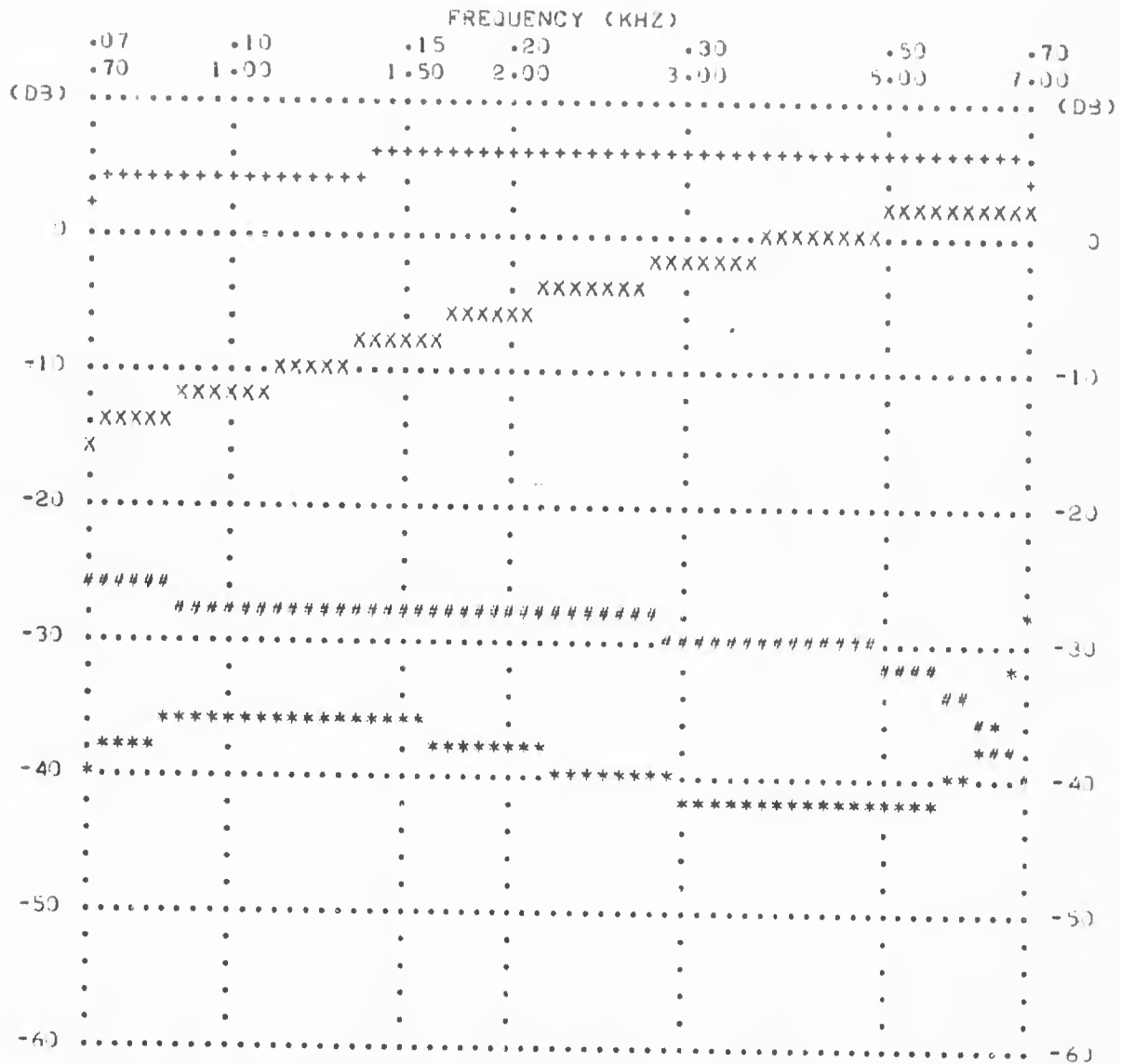
UPPER/LEFT SCALES
FROM FRONT]
FROM BACK [

LOWER/RIGHT SCALES
FROM FRONT >
FROM BACK <

Figure 4-2. Computed Performance of Spring-Mass
Baffle (Compliant Outer Plates) (Sheet 3 of 4)

PRESSURE AT FRONT OF
MOUNTED BAFFLE CONFIGURATION
(DB//INCIDENT WAVE)

	PIN SPACE 3.00									
	WATER GAP 2.00									
MASSES	.0233	.0466	.0512	.0233	.0395	.0233	.0512	.0466	.0233	4.4145
SPRINGS	800	800	800	800	800	800	800	800		
DAMPING	.05	2.40	2.40	2.40	2.40	2.40	2.40	.05		



UPPER/LEFT SCALES
FROM FRONT X
FROM BACK #

LOWER/RIGHT SCALES
FROM FRONT +
FROM BACK *

Figure 4-2. Computed Performance of Spring-Mass
Baffle (Compliant Outer Plates) (Sheet 4 of 4)

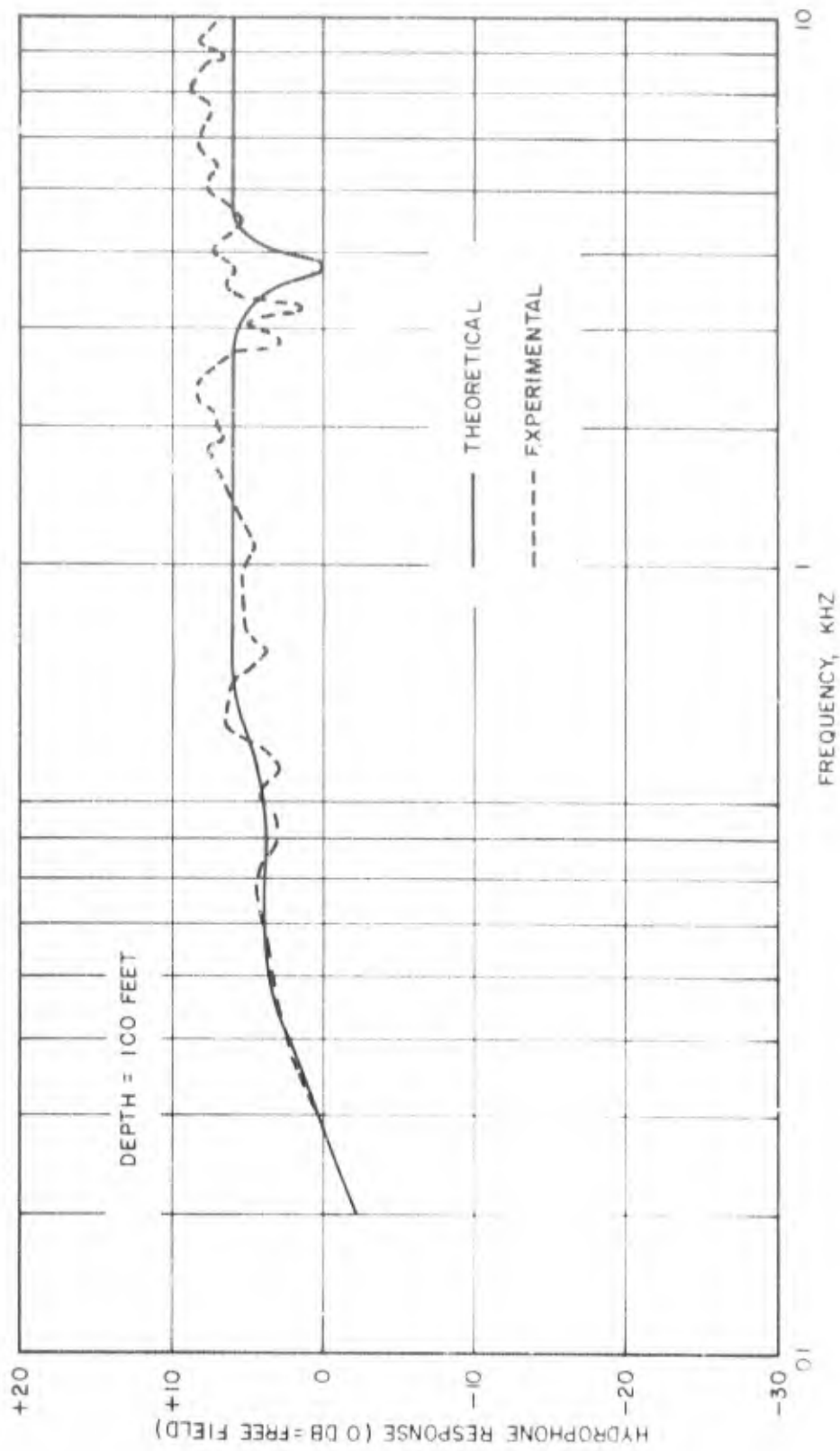


Figure 4-3. Comparison of Computed and Experimental Baffled Hydrophone Response (Depth = 100 Feet)

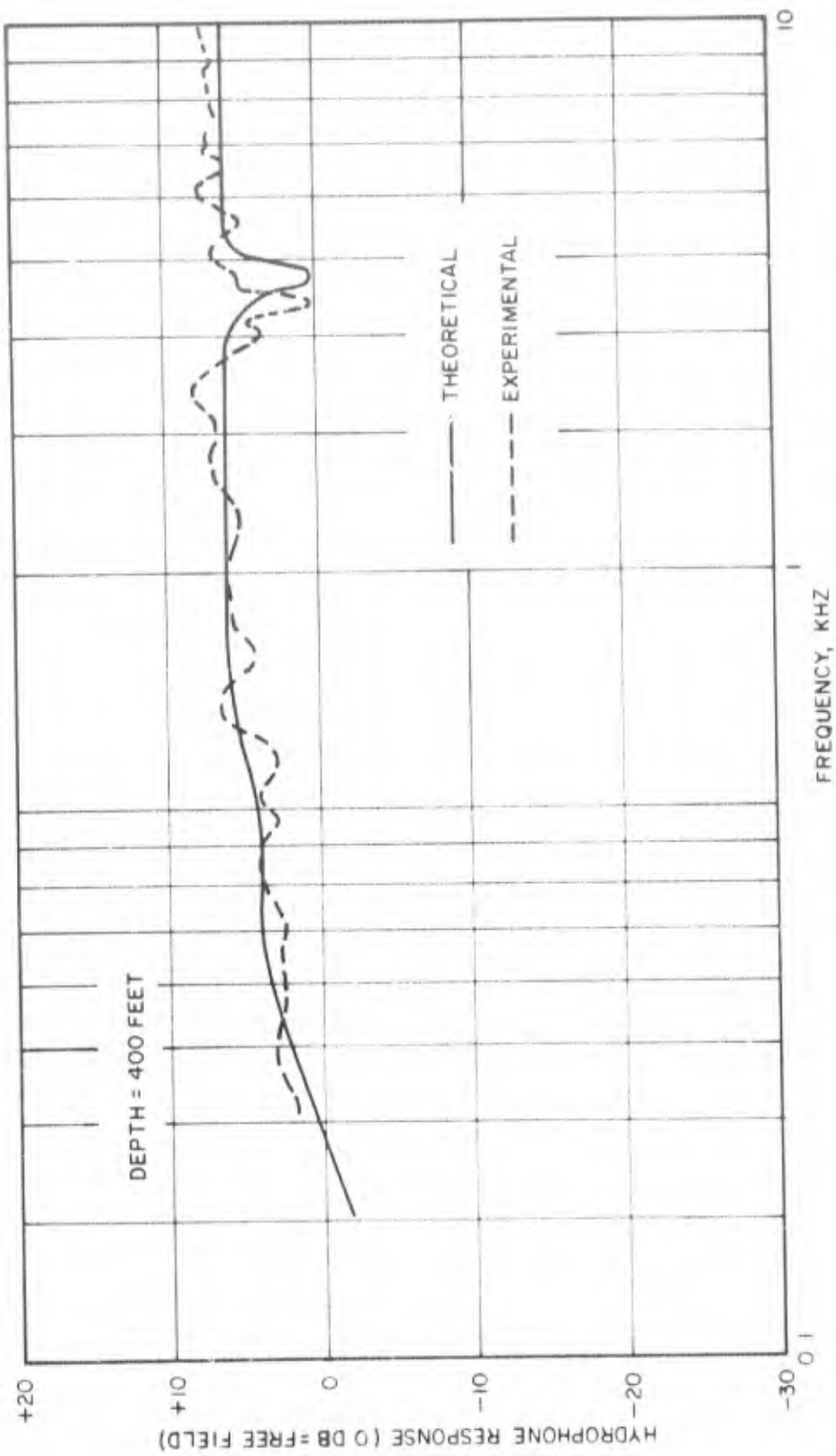


Figure 4-4. Comparison of Computed and Experimental Baffled Hydrophone Response (Depth = 400 Feet)

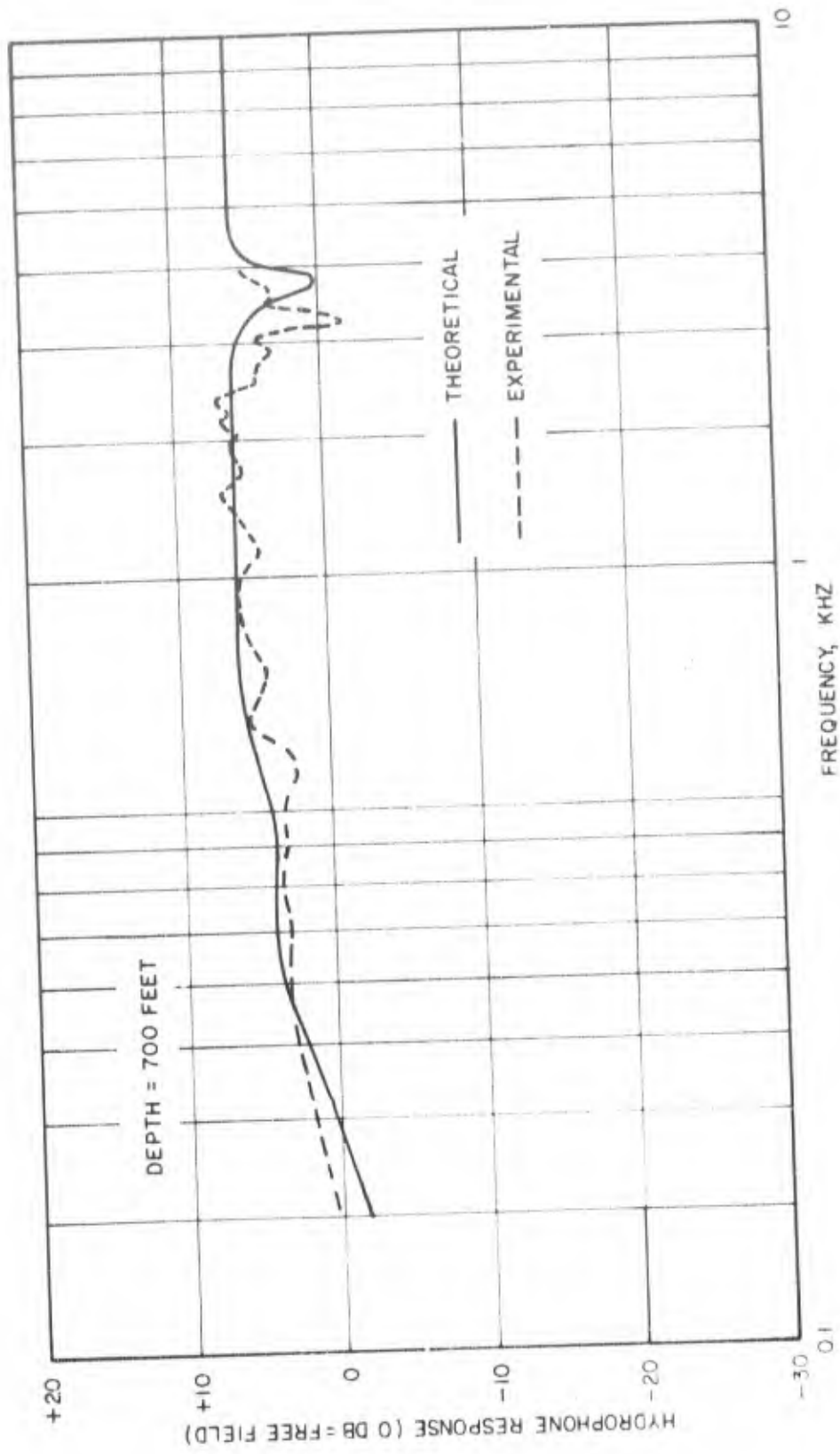


Figure 4-5. Comparison of Computed and Experimental Baffled Hydrophone Response (Depth = 700 Feet)

SECTION 5

REFERENCES

1. Underwater Acoustic Noise Reduction Program-Interim Report, Sperry Gyroscope Division, SGD-4232-0014, April 1968.
2. Underwater Noise Reduction Study-Interim Report Phase II, Sperry Gyroscope Division, SGD-4232-0225, April 1969.
3. Analysis of Acoustic Baffles for Underwater Noise Reduction, Sperry Gyroscope Division, SGD-4230-0430, June 1971.

UNCLASSIFIED

Security Classification

DOCUMENT CONTROL DATA - R & D

Security classification of title, body of abstract and indexes, annotation must be entered when the overall report is classified

1. ORIGINATING ACTIVITY (Corporate authority) Sperry Gyroscope Division Sperry Rand Corporation Great Neck, N. Y. 11020	2a. REPORT SECURITY CLASSIFICATION Unclassified
	2b. GROUP None

3. REPORT TITLE
ANALYSIS OF ACOUSTIC BAFFLES FOR UNDERWATER NOISE REDUCTION

4. DESCRIPTIVE NOTES (Type of report and inclusive dates)

5. AUTHOR (S) (First name, middle initial, last name)
Brian E. Owens, George Rand, Barry Schwartz

6. PERIOD DATE December 1971	7a. TOTAL NO. OF PAGES 41	7b. NO. OF FIGS. 3
--	-------------------------------------	------------------------------

8a. CONTRACT OR GRANT NO. N00014-67-C-0303	9a. ORIGINATOR'S REPORT NUMBER(S) SGD-4230-0476
8b. PROJECT TITLE	9b. OTHER REPORT NUMBER: (Give other numbers that may be assigned this report)

10. DISTRIBUTION STATEMENT
Distribution limited to U. S. Government agencies only; Test and Evaluation; 21 December 1971. Other requests for this document must be referred to Chief, Office of Naval Research, Attn: Code 468, Arlington, Va. 22217.

11. SUPPLEMENTARY NOTES	12. DISTRIBUTION STATEMENT Department of the Navy Office of Naval Research Acoustic Program (Code 468) Washington, D. C. 20360
-------------------------	--

14. ABSTRACT

This is an interim report on the study of underwater noise reduction techniques being conducted by the Sperry Division for the Office of Naval Research, Acoustic Programs, under Contract No. N00014-67-C-0303. Included in this report is a description of the work being done on spring-mass type acoustic baffles. Specifically, the effects of rigid and compliant outer plates are analyzed, theoretical results are compared with experimental data, and good agreement is obtained. It is concluded that significant gains can be achieved at the lower frequencies through the use of compliant outer plates in the baffle design.

UNCLASSIFIED

Security Classification

14 KEY WORDS	LINK A		LINK B		LINK C	
	ROLE	WT	ROLE	WT	ROLE	WT
Acoustic baffles Waterborne noise reduction						

DISTRIBUTION LIST

	No. of Copies
Office of Naval Research Navy Department Arlington, Virginia 22217	
Code 468	2
Code 439, Dr. Nicholas Perrone	1
Director, U. S. Naval Research Laboratory Attn: Technical Information Division Washington, D. C. 20390	6
Commanding Officer and Director Naval Ship Research and Development Center Washington, D. C. 20007	
Attn: Dr. W. S. Cramer, Code 945	1
Mr. Nathan Gaynor, Code 926	1
Officer in Charge Annapolis Division Naval Ship Research and Development Center Annapolis, Maryland 21402	1
Commanding Officer and Director U. S. Naval Underwater Systems Center New London, Connecticut 06321	
Attn: Mr. Walter Clearwater	1
Dr. Charles H. Sherman	1
Director, Defense Documentation Center Cameron Station Alexandria, Virginia 22314	20
Ordnance Research Laboratory Pennsylvania State University University Park, Pennsylvania 16801	
Attn: Dr. John C. Johnson	1

DISTRIBUTION LIST (Cont'd)

	No. of Copies
Commander Naval Ship Systems Command Navy Department Washington, D. C. 20360	
Attn: Code 0372	1
CDR R. B. Gilchrist, Code 902	1
Carey D. Smith, Code 901	1
Code PMS 386	1
 General Dynamics/ Electric Boat Division Eastern Point Road Groton, Connecticut 06340	 1
 Dr. Philip Stocklin Raytheon Company P. O. Box 360 Newport, Rhode Island 02841	 1
 Dr. Preston Smith, Jr. Bolt Beranek and Newman, Inc. 50 Moulton Street Cambridge, Massachusetts 02138	 1
 Dr. Frank Andrews The Catholic University of America Washington, D. C. 20017	 1
 Dr. Douglas Muster University of Houston Department of Mechanical Engineering 3801 Cullen Boulevard Houston, Texas 77004	 1
 Mr. Sam Hanish Code 8150 Naval Research Laboratory Washington, D. C. 20390	
 H. V. Hillery Applied Research Laboratories University of Texas at Austin Austin, Texas 78712	 1

46